Biophysical Chemistry 125 (2007) 368–374

Biophysical Chemistry

http://www.elsevier.com/locate/biophyschem

Voltage regulation of single green fluorescent protein mutants

Fabio Cannone [a,d], Roberto Milani [a,d], Giuseppe Chirico [a,d,*], Alberto Diaspro [b,d,e], Silke Krol [b,d], Barbara Campanini [c,d]

[a] Department of Physics, LABS, University of Milano Bicocca, Piazza della scienza 3, 20126 Milano, Italy
[b] LAMBS, MicroScoBiO Research Center and Department of Physics, University of Genoa, Via Dodecaneso 33, 16146 Genova, Italy
[c] Department of Biochemistry and Molecular Biology, University of Parma, 43100 Parma, Italy
[d] INFM-CNR Istituto Nazionale per la Fisica della Materia and Centro Nazionale delle Ricerche, Italy
[e] IFOM, FIRC Institute for Molecular Oncology Foundation, Via Adamello, 16, 20139 Milan, Italy

Received 29 August 2006; received in revised form 25 September 2006; accepted 25 September 2006
Available online 5 October 2006

Abstract

We report the analysis of the fluorescence intensity fluctuations of single proteins of a GFP mutant, GFPmut2, embedded in a polyelectrolyte nanocapsule adsorbed on thin conductive layers. Our results, based on single molecule fluorescence spectroscopy, indicate that the fluorescence blinking dynamics of GFP is strongly dependent on the bulk conductivity of the metal layer substrate, on the distance from the conductive surfaces and on the amplitude of the voltage applied to the poly-electrolyte layers. These findings suggest that fluorescence blinking itself might be employed as a reporter signal in nano-bio-technology applications.

Keywords: Fluorescence; Blinking; Green Fluorescent Protein; Voltage regulation; Microscopy

1. Introduction

The interest in sensors based on biological molecules, DNA and proteins, have seen an upsurge in these years [1,2]. A crucial aspect in the realization and optimization of future opto-electronic bio-molecular devices is the connection between the molecules and the macroscopic (semi-)conductor components that transmit energy to more traditional components [3,4] and how this affects the molecular optical response. Devising a sensor requires therefore the characterization of the biomolecule response, mostly fluorescence, in vitro and on the sensor surface.

In particular fluorescence blinking (reversible loss of fluorescence) [5], switching between two emission colors [6,7] and bleaching (irreversible loss of fluorescence) [8] are among the most frequent sources of dynamics in the optical signal. Single-Molecule Spectroscopy (SMS) [9–11] has emerged as an important method for the study of the fluorescence dynamics [12,13] and, through this, of the conformational or chemical dynamic processes in molecules [14–16]. SMS is particularly well suited for the study of low quantum yield excited-state deactivation processes.

Among proteins, Green Fluorescent Protein (GFP) and its mutants appear to be particularly well suited for bio-sensor applications [17]. GFP mutants show randomly distributed events of reversible loss of fluorescence emission [5,8], that are ascribed to a conversion between the bright anionic (HO_Y,HN^+, O_X) and the dark zwitterionic (O_Y^-,HN^+,O_X) form of the chromophore [17–19]. GFP can also switch between the anionic and the neutral form of the chromophore, yielding anti-correlated signals at two distinct emission wavelengths [7]. Various trapping methods have been proposed for SMS of GFP, from poly(acrylamide) gels [5,6] to silica gels [20,21]. Nanocapsules (NC), fuzzy assemblies of multilayered polyelectrolyte films [22,23] with an amorphous core, represent an alternative trapping method, and offer new challenging opportunities to the preparation of molecular electronics devices.

This manuscript reports the analysis of the fluorescence intensity fluctuations of a complex system composed by a GFP mutant, GFPmut2 [8,21,24,25], embedded and observed at single molecule level in a polyelectrolyte nanocapsule adsorbed

* Corresponding author.
E-mail address: giuseppe.chirico@unimib.it (G. Chirico).

0301-4622/$ - see front matter © 2006 Elsevier B.V. All rights reserved.
doi:10.1016/j.bpc.2006.09.012

on surfaces of varying conductivity. Blinking, switching and spectral diffusion of the fluorescence emission of different GFP mutants have been previously reported [5–8,13,17]. The novelty of the present report lies in the analysis of the fluorescence blinking dynamics of GFP close to conductive surfaces. The data reported here show that the GFP emission blinking rate depends linearly on the bulk conductivity of the surfaces and the voltage applied to the nanocapsule layers. These results suggest that fluorescence blinking itself might be employed as a reporter signal in nano-bio-technology applications.

2. Materials and methods

2.1. Nanocapsule preparation

The nanocapsules are built by adsorption of positive and negative charged polyelectrolyte onto carbonate templates [23,26,27]. Poly(styrenesulfonate sodium salt) (PSS, MW 70 000 Da, Aldrich) and poly(allylamine hydrochloride) (PAH, MW 15000 Da, Aldrich) are dissolved in 0.5 M NaCl at a concentration of 2 mg/mL in Milli-Q-grade water. Each of the six steps of polyelectrolyte adsorption onto a spherically shaped calcium carbonate core (≅4.7 μm in diameter) [23], is performed by incubation in the proper polyion solution (5 min for PAH, 10 min for PSS) followed by two steps of centrifugation and washing in 0.5 M NaCl. This procedure leads to spherical nanocapsules with six layers (≅2 nm/layer) [28]. Fluorescent nanocapsules are obtained by adding a small aliquot of a 10 nM GFPmut2 solution (volume ratio=1/100) to the nanocapsule solution between the fifth and sixth step of polyelectrolyte adsorption.

2.2. GFPmut2 mutant

GFPmut2 is a mutant of GFP containing a triple substitution (S65A, V68L, S72A) responsible for an enhanced fluorescence emission [24,25]. GFPmut2 gene, cloned in a pKEN1 vector, was kindly provided by Dr. Brendan P. Cormack (Department of Microbiology and Immunology, Stanford University School of Medicine, Stanford, CA) [24]. Protein expression and purification was carried out as previously described [25]. GFPmut2 stock solutions were dialyzed against 50 mM Tris buffer, pH 8.0, and kept at −80 °C.

The Two Photon Excitation (TPE) spectrum of single GFPmut2 molecules encapsulated in silica gels exhibits two main components at 820±2 and 885±3 nm [8]. The excitation at 885 nm is largely favored at high pH with respect to the band at 820 nm, suggesting that the 885 nm excitation band is due to the two-photon absorption of the anionic state of the GFPmut2 chromophore, while the excitation at 820 nm corresponds to the absorption of the neutral chromophore. The single molecule TPE emission spectrum, upon excitation at 820 nm, shows two bands at 450 and 510 nm, [8] in good agreement with the one photon emission spectra. At basic pH, the component at 510 nm

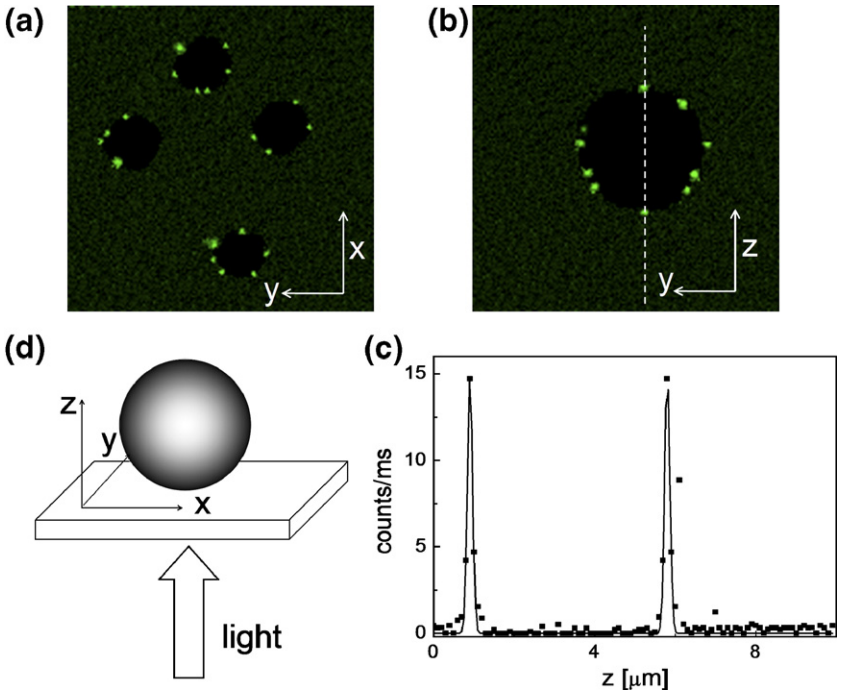

Fig. 1. Fluorescence images of GFPmut2 absorbed on nanocapsules. *Z* axis is the optical axis, while *x* and *y* axes are in the plane perpendicular to the *z* axis. (a) Fluorescent spots assigned to the emission of single GFPmut2 or small aggregates adsorbed between the PSS–PAH layers in a nanocapsule at $z \cong 2.4$ μm from the contact point between nanocapsule and glass surface along the optical axis. The field of view is 25×25 μm^2. Excitation intensity is $I_{exc} \cong 10$ kW/cm^2. (b) Fluorescent spots assigned to GFPmut2 proteins adsorbed between the PSS–PAH layers in a nanocapsule. The field of view is 10×10 μm^2. This image represents an axial section of the capsule in the bottom of panel a. (c) Fluorescence signal acquired versus the distance from the glass slide along the *z* axis along the dashed line in panel b. The solid line is the best fit of the data to a sum of two Gaussian functions. (d) Sketch of a nanocapsule adsorbed on the glass slide: *z* axis is the optical axis.

is largely favored and it is ascribed to the anionic state of the GFPmut2 chromophore. The emission at ≅460 nm is due to the neutral state of the chromophore [8].

The optical absorption and fluorescence properties of GFP are commonly described in terms of three chemical states of the chromophore [8,17]: a neutral (protonated), an anionic (deprotonated) and a zwitterionic dark state [19]. Excitation at 885 nm (anionic component) gives rise to fluorescence emission blinking that is due to a transition between the anionic to the zwitterionic form of the GFP chromophore [17].

2.3. Metal layers preparation

In order to have free charge surfaces, high concentration (900 μM) metal salts were spin coated at 2000 rpm on clean glass slides [25,29]. For this purpose we have used: silver nitrate (54,501-5, Aldrich), mercury nitrate monohydrate (51,365-3, Aldrich), aluminum nitrate monohydrate (23,797-3, Aldrich), copper(II) nitrate hydrate (22,963-6, Aldrich), iron(III) nitrate monohydrate (52,930-3, Aldrich) and gold colloid (20 nm diameter, G1652, Aldrich). Alternatively the fluorescent nanocapsules are absorbed directly on a quartz or mica surface. All glass and quartz surfaces have been treated with chemical etching agents prior to metal deposition [8].

2.4. Fluorescence microscope setup

Single-molecule fluorescence images and traces are collected on a two-photon scanning microscope [30], in which a tightly focused laser spot (~200 nm) is used to excite one molecule at a time. The single molecule emission was detected by a single photon avalanche diode module (SPCM-AQR-14, Perkin Elmer, Canada). The laser light at 880 nm (80-MHz pulse repetition, pulse width ≅280 fs on the sample) was circularly polarized. The emission coming from the anionic state only was selected by a band pass filter (HQ515/30 nm, Chroma, Rockingham, VT, USA) [8].

2.5. Fluorescence imaging

Fluorescence imaging has been obtained with 1 ms dwell time, 150 nm pixel size, typically on 25×25 μm^2 fields of view. The excitation intensity on the sample was ≅10 kW/cm^2 [8].

3. Results and discussion

3.1. Nanocapsule images

The nanocapsule images are characterized by a dark core (fluorescence signal 0.05±0.03 kHz) surrounded by few discrete fluorescence spots, that we ascribe to single proteins according to their single step bleaching as described in detail elsewhere [8]. A scan in the optical axis direction indicates that the dark core thickness is 5.0±0.3 μm, similarly to the size evaluated by means of Atomic Force Microscopy [22]. Single GFPmut2 molecules bind at different positions on the nanocapsule surfaces and therefore at different distances from the glass surface (Fig. 1).

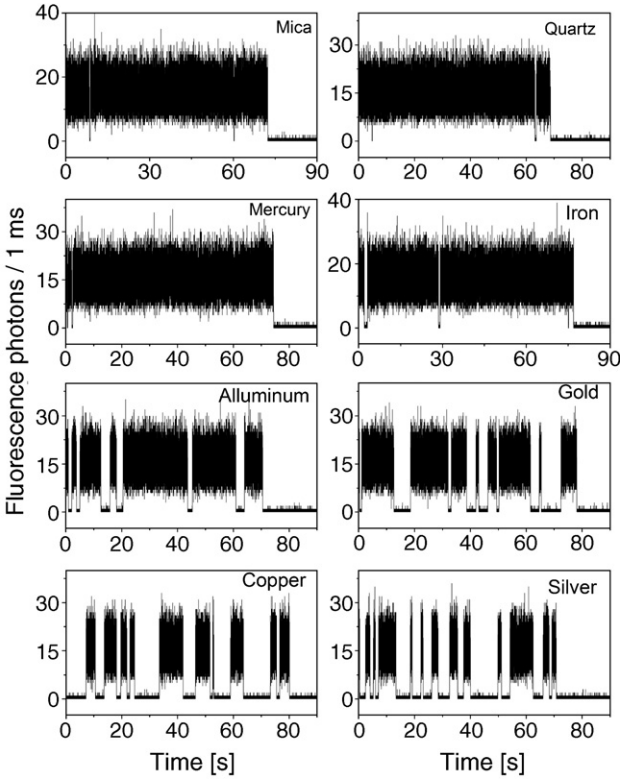

Fig. 2. Fluorescence traces of single GFPmut2 proteins in anionic state (λ_{ex}=880 nm, λ_{em}=515±15 nm, I_{exc}=10 kW/cm^2, sampling time 1 ms) absorbed between PSS–PAH layer of a nanocapsule at z≅0 nm from the surface. The metal deposited on the glass slide is Mica, Quartz, Mercury, Aluminum, Iron, Gold, Copper and Silver, as indicated in the panels.

3.2. GFPmut2 photodynamics on nanocapsules

Typical fluorescence traces collected from single GFPmut2 molecules show several blinking events (Fig. 2), or reversible losses of fluorescence up to the time, T_{BL}, at which bleaching occurs [8]. Single proteins alternate therefore between a bright and a dark state that correspond to 0.3±0.2 photons/ms, close to the image background (the "off" state), and 14±3 photons/ms, which is the level of fluorescence for a single GFPmut2 in anionic state as observed in hydrated matrices [8]. We have found no clear dependence of the single molecule brightness in the bright state and the bleaching time [8] on the type of metal deposited on the surfaces, and we have verified that the dark time spans observed at λ_{em}=515±15 nm do not correspond to a spectral shift (in the range 400–610 nm), i.e. to switching events between states with different fluorescence yields. Similar results have been obtained by means of single photon excitation (excitation wavelength 488 nm) on a confocal setup.

The blinking dynamics can be described in terms of the on-time (t_{on}) and the off-time (t_{off}), defined as the lifetime of the bright and dark states, respectively [31]. The probability distributions of the on- and off-times are well described by single-exponential curves whose decay time provides the average lifetimes of the "on" and "off" states (Fig. 3a,b,c,d) [5,31,32], $<t_{on}>$ and $<t_{off}>$.

As expected for the two-photon excitation mode employed here [8], we have found a quadratic dependence of the average

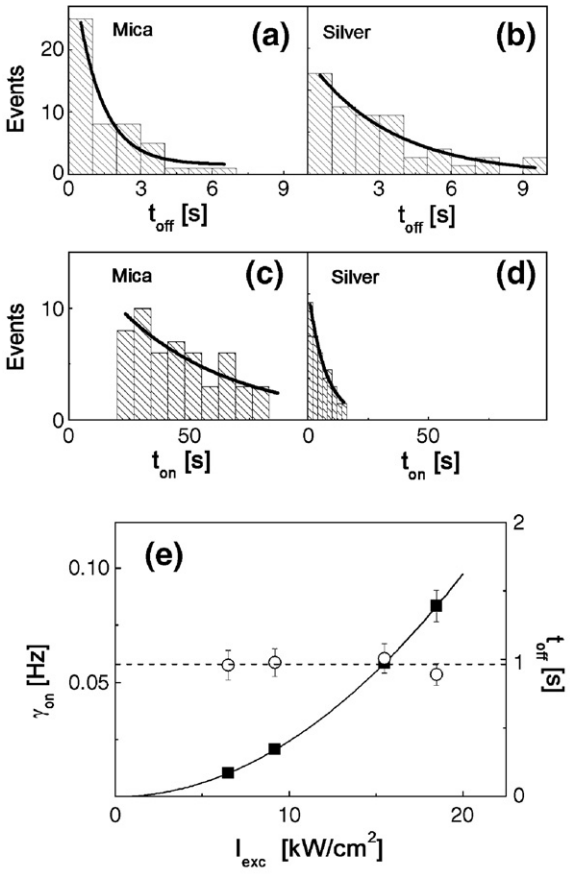

Fig. 3. Histogram of the t_{on} and t_{off} times evaluated by analyzing about 100 single GFPmut2 absorbed on the PSS–PAH nanocapsule at $z \cong 0$ nm from the metal coated surface. The solid line represents a mono-exponential best fit to the data. Panel a and c report the t_{on} and t_{off} data for the case of nanocapsules deposited on Mica. Panel b and d report the t_{on} and t_{off} data for the case of nanocapsules deposited on Silver. Panel e: average t_{off} times (right axis) and average on-rate $\gamma_{on}=1/<t_{on}>$ (left axis) versus the excitation intensity for GFPmut2 proteins at $z \cong 0$ from a Mica layer. The dashed line is the best fit linear fit to the t_{off} data. The solid line is the best fit of the γ_{on} data to the function $\gamma_{on}=\alpha I_{exc}^2$.

blinking frequency $\gamma_{on}=1/<t_{on}>$ of GFPmut2 on the excitation intensity (a linear dependence has been found when employing single photon excitation on a confocal setup). On the contrary, $<t_{off}>$ does not depend appreciably on the excitation intensity (Fig. 3e). Fluorescence blinking is therefore a photo-activated transition to a non-fluorescent state, probably the zwitterionic form of the GFP chromophore [17–19]. The observed blinking should not be ascribed to a photo-conversion to the other bright states [7], since no emission at other wavelengths in the range 400–610 nm has been observed upon transition to the dark state at 515 nm. It could not either be ascribed to translational diffusion, since repeated fluorescence images over the same area and over time periods from minutes to hours reveal no change in the positions of the molecules.

3.3. Blinking dynamics depends on the metal conductivity

Blinking dynamics depends on the type of metal deposited on the glass surface, as can be seen from Fig. 2. If blinking can be ascribed to a photo-activated transition between the anionic and the zwitterionc state [17–19], that implies a protonation of the chromophore, its dependence on the properties of the metallic layer, might be due [31] to fluctuations in the local concentration of ions (likely protons) induced by the contact between the metallic surface and the nanocapsule. The molecule stops fluorescing when it takes an electron from the surface, and remains in the "off" state, i.e. in the zwitterionic form, until the electron returns to the surface and the molecule comes back to the "on" state, i.e. in the anionic from, thereby resuming fluorescence emission.

Interestingly a single parameter describe the blinking dependence on the metal properties. The average rate $\gamma_{on}=1/<t_{on}>$ and the average off-time, $<t_{off}>$, scale linearly with the *bulk* conductivity σ of the metal (Fig. 4). In particular the extrapolated value at $\sigma \cong 0$ are $<t_{off}>=1.1\pm0.2$ s and $\gamma_{on}=0.02\pm0.004$ Hz. If the electron donor is an insulating surface (Quartz or Mica) $<t_{off}>$ is very close to that measured for single GFPs embedded in a six layers PSS–PAH (inset Fig. 4) film deposited on a glass slide: the blinking event is very unlikely in these conditions.

According to the simple Drude model [33], metal conductivity is given by the product of the volume density of the charge carriers times their mean free-path time, $\sigma \cong n_q \tau$. It is possible that the close contact of the metal layer and the polyelectrolytes induces a local redistribution of charges at the interface, that results in a local increase of concentration of protons (equilibrated by electrons injected by the metal layer into the nanocapsule) in the polyelectrolyte. It is noteworthy and surprising that this effect can be described by a linear dependence on the single parameter σ, which is related to metal bulk properties.

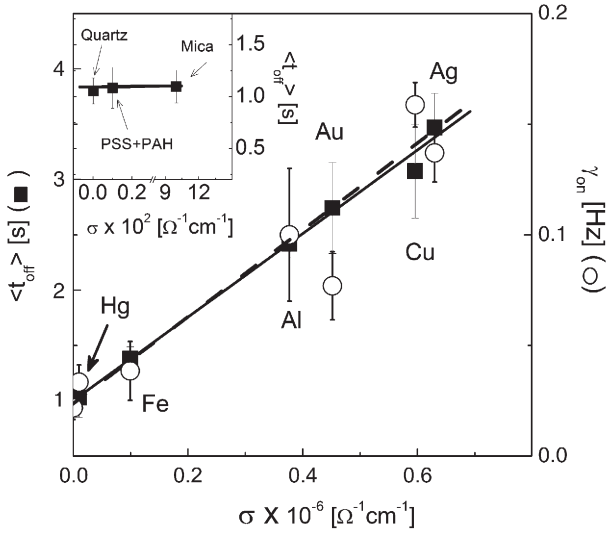

Fig. 4. Blinking dependence on metal bulk conductivity, σ. Left axis: $<t_{off}>$ versus σ of the metal spin coated measured from ≅100 single GFPmut2 proteins at close contact to the metal layer ($z \cong 0$). The solid line $<t_{off}>=A+\sigma B$, where $A=1.0$ (±0.1) s and $B=3.7$ (±0.5)$\times10^{-7}$ s Ω cm, represents the best fit of the data. Inset: dependence of the off-time on σ on insulating surfaces. Right axis: rate of the blinking transition, $\gamma_{on}=<t_{on}>$, versus σ. The solid line $\gamma_{on}=A+\sigma B$, where $A=0.024$ (±0.008) Hz and $B=2.0$ (±0.2)$\times10^{-8}$ Hz Ω cm, represents the best fit of the data. The uncertainties in the best fit values correspond to the standard errors.

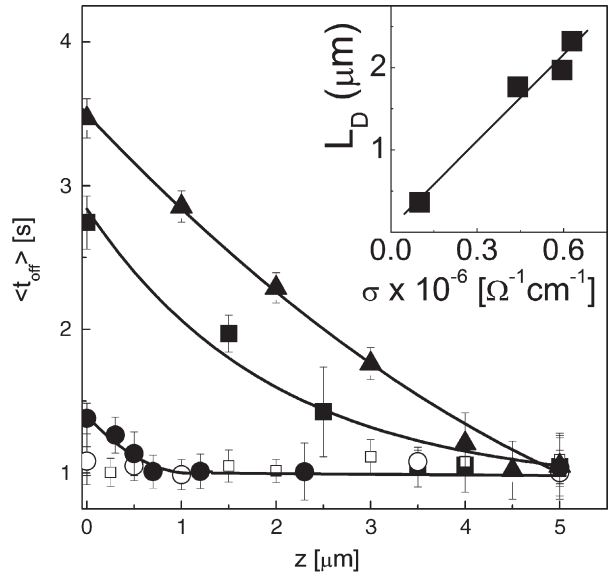

Fig. 5. $<t_{off}>$ versus the distance of single GFPmut2 proteins from Mica (open circles), Quartz (open squares), Iron (filled circles), Gold (filled squares) and Silver (filled triangles) surface in absence of an external bias. When the nanocapsules are deposited on mica or quartz, $<t_{off}>$ shows negligible dependence on z. The solid lines are best fit of the data to single exponential decays. Inset: the best fit decay length, L_D (see text).

3.4. Blinking dynamics depends on the GFP-metal distance

The fluorescence blinking of GFPmut2 proteins also varies substantially with the protein-layer distance, z (Fig. 5). In particular $<t_{off}>$ decreases versus z (with an opposite trend of $<t_{on}>$) from a value $<t_{off}>_0$ (measured at $z \cong 0$, the contact point of the NC onto the metal layer) that depends on the metal layer conductivity, to a limiting value $<t_{off}>_\infty$ (Fig. 5). This limiting value is common to the whole series of metals investigated and equals the value of the off-time measured for GFP embedded in polyelectrolyte layers spread on glass. The trend of $<t_{off}>$ versus z is well described by an exponential decay of the type $\langle t_{off}\rangle = \langle t_{off}\rangle_\infty + (\langle t_{off}\rangle_0 - \langle t_{off}\rangle_\infty)e^{-z/LD}$. The decay length, L_D, scales linearly with the metal conductivity σ (inset Fig. 5).

For an interface between an organic layer and a metal surface, band bending in the organic layer should be considered. Work functions for the metal and the organic layer are different and soon after contact a charge redistribution around the interface takes place. Some electrons may move from the organic layer to the metal and this movement leads to a negative charging of the metal and an opposite charging of the organic layer. This double layer induces a depletion layer and an additional potential V_b in the organic layer that, summed to its energy band structure leads to an equilibration of the Fermi level of the organic layer to that of the metal. The thickness of the depletion layer is related to the Debye Hückel length for the organic layer, L_D [34], and the interface potential V_b [35] by the relation: $W = L_D\sqrt{2(V_b/K_BT - 2)}$.

The Debye–Hückel length is $L_D \cong \left(\frac{\varepsilon\varepsilon_0 K_B T}{q^2 n_I(0)}\right)^{0.5}$ where ε_0, K_B, T, and q are the vacuum dielectric permittivity, the Boltzman constant, the temperature and the electron charge, respectively. $n_I(0)$ is the concentration of the excess ions present at the polyelectrolyte–metal interface due to the charge injection from the metal.

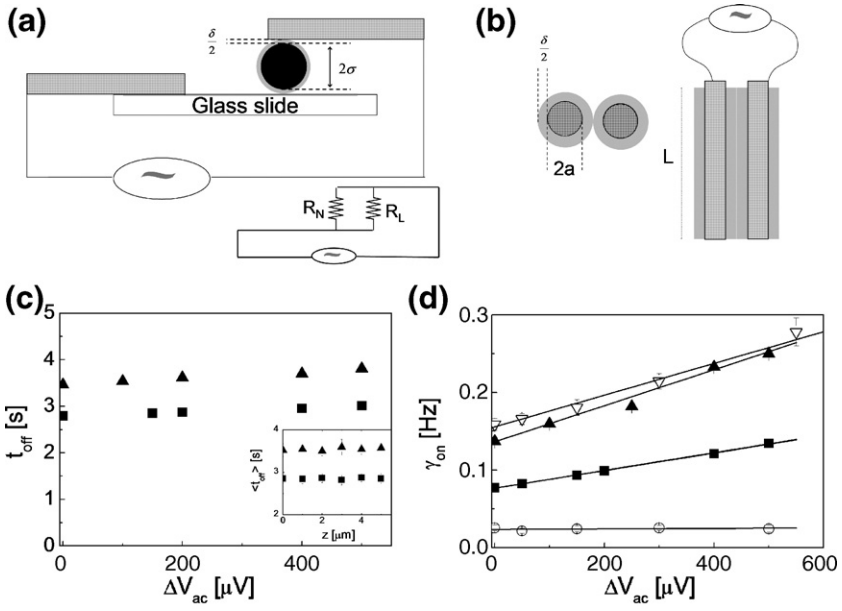

Fig. 6. (a) Sketch of the circuit used to apply an alternating (1 kHz) voltage on the nanocapsules. Two platinum electrodes are touching the metal layer and the nanocapsule respectively. The polyelectrolyte layers amount to $\delta/2$ in thickness and the core diameter is σ. Lower sketch represents the scheme of the circuit with the nanocapsule (R_N) and the leakage (R_L) resistance. (b) Sketch of the circuit used to estimate the polyelectrolyte layers resistivity. Two platinum electrodes (radius = a) are layered with polyelectrolytes as done for the nanocapsule and kept into contact over a length L. (c) The average off time $<t_{off}>$ measured on single GFPmut2 proteins on the nanocapsules at close contact to the metal layer surface ($z \cong 0$) for Gold (filled squares) and Silver (filled up triangles) in presence of an external alternating bias applied between two platinum electrodes as shown in the sketch a. Inset: $<t_{off}>$ versus the distance along the optical axis from the metal layer for the case $\Delta V_{ac} = 200$ μV. (d) The on rate $\gamma_{on} = 1/<t_{on}>$ versus the external alternating bias for Copper (open triangles), Gold (filled squares), Silver (filled triangles) and Mica (open circles). Solid lines are best linear fit to the data.

According to the Poisson–Boltzman model [34] of the spatial organization of free charges (in the polyelectrolyte) around a fixed charge distribution (on the metal–polyelectrolyte interface), we expect an exponential decay, $n_I(s) \cong n_I(0)e^{-s/W}$, of the effective charge density of the ions, $n_I(s)$, in the polyelectrolyte layers with the distance from the metal surface, s. V_b is typically of the order of 1–5 V [35] and therefore $W \cong 8$–$10\ L_D$. By assuming a polyelectrolyte dielectric permittivity $\varepsilon \cong 2$ [36], we can then predict decay lengths of the order of micrometers as observed here, if the ionic density at the interface $n_I(0) \cong 400$ nM. These decay lengths agree with the prediction of the charge diffusion layer at the metal–organic interface [35]. Moreover the predicted local concentration of ions corresponds to an absolute number of charges injected in the organic layer ≅ 40–120 (as computed for a concentration $n_I(0)$ in a portion of the nanocapsule that corresponds to an arc ≅1–3 μm in length and ≅12 nm in thickness).

From the application point of view, the main question regarding the observed blinking behavior of GFPmut2 proteins, is whether fluorescence blinking depends on the charge density current or on local voltage or current fluctuations. We have then followed the fluorescence dynamics of single GFPmut2 proteins embedded in the nanocapsule, while applying an alternate voltage (frequency 1 kHz) between the metal surface and the nanocapsule itself. The voltage has been applied between two platinum electrodes (diameter = 2 $a \cong 0.1$ mm) placed on the top of a single nanocapsule (Fig. 6a). Due to the small size of the nanocapsule compared to the platinum electrodes, leakage of the current between the top electrode and the metal layer is not avoidable. Leakage sources may be due, for example, to a small hydration layer (of micrometer thickness) between the metal layer and the top platinum electrode. The system can then be modeled as a parallel of two resistor, R_L and R_N, due to the leakage contact and to the nanocapsule itself (Fig. 6a).

We have evaluated the resistivity of the six polyelectrolyte layers by measuring the electrical resistance between two polyelectrolyte layered platinum electrodes (Fig. 6b). The resistance measured under ac bias (1 kHz) is $R \cong 1$ MΩ. Since the contact length between the electrodes is $L \cong 10$ mm and the polyelectrolyte layer is $\delta/2 \cong 12$ nm in thickness, much less than the electrode radius $a \cong 0.1$ mm, the estimated resistivity of the polyelectrolyte layer is $\rho \cong R(aL)/\delta \cong 10^{10}$ Ω cm. The nanocapsule resistance R_N can then be estimated as that of a sheet with thickness $\delta/2$, height $\pi\ r_N$ ($r_N \cong 5$ μm is the nanocapsule radius) and length $\cong \pi\ r_N$, resulting in $R_N \cong \rho/\delta \cong 10^{16}$ Ω. Even by assuming the nominal resistivity of MilliQ™ water (Millipore, resistivity ≅ 20 MΩ cm) used in the experiments (additional salts should also be present in the nanocapsule solutions), the resistance of the hydration layer (100 μm × 1 mm, 5 μm thick) responsible for the leakage current (Fig. 6a) should be much less than the nanocapsules itself, i.e. $R_L \cong 10$ MΩ $\ll R_N$. The resistance actually measured in the circuit is of the order of few Ohms and depends on the metal deposited on the glass slide. This is an indication that most of the leakage current is actually passing through direct electrode-metal layer contacts, which cannot be avoided due to the small size of the nanocapsules. We can therefore assume that almost no current is passing through the layers of the capsule itself.

The off-time increases linearly with the peak-to-peak voltage, ΔV_{AC}, up to ≅ 10% of the value measured under no external bias (Fig. 6c). On the contrary the on-rate, γ_{on}, doubles when increasing ΔV_{ac} to ≅ 500 μV (Fig. 6d). This implies that the change in the blinking frequency (or γ_{on}) might be employed as a parameter for sensing tiny voltages at molecular level by means of a fluorescent protein, GFP. Finally we notice that the slope of γ_{on} versus ΔV_{ac} is approximately the same for all the metal layers, and is likely to depend on the GFP protein itself and/or the tiny resistivity of the polyelectrolyte composing the nanocapsules. The absolute value of the blinking frequencies, on the other hand, depends on the donor system, the metal layer, and scales with its conductivity as found in absence of an external bias.

4. Conclusions

Average fluorescence blinking rates of the order of 0.1–1 Hz have been measured on single GFPmut2 proteins depending on the distance of the proteins from thin layers of metals. In addition, the GFPmut2 blinking rate, γ_{on}, depends linearly on the bulk metal conductivity. Moreover, an alternating applied voltage of the order of few tens of μVolts induces a measurable increase in the blinking frequency. Although these results have been obtained by single molecule two-photon fluorescence, very similar behavior can be retrieved by single photon excitation on a confocal setup. These observations suggest the possibility to develop molecular voltmeters systems based on the measurement of the fluorescence blinking frequency of GFP. To this purpose specific mutants should be devised in order to amplify the observed blinking frequency dependence on the applied voltage and to increase the blinking frequency.

Specifically designed GFP mutants might be embedded in a highly insulating matrix that could act as a nano-chip able to measure tiny voltages with optical microscopy resolution. Moreover, we should consider that GFP can be engineered with other proteins thereby obtaining hybrid constructs that can be tailored to tag specific sites in widely diverse living systems. The properties studied here could be exploited in such GFP constructs in order to have a molecular device able to measure voltage drops inside living cells or within cell membranes.

Acknowledgments

This research has been funded by PRIN 2004-2005 to A.D. and G.C. and by the “Optical Molecular Memories” project 2006–2007 by Fondazione Cariplo to G.C.

References

[1] M. Sauer, Single-molecule-sensitive fluorescent sensors based on photoinduced intramolecular charge transfer, Angew. Chem., Int. Ed. 42 (2003) 1790–1793.
[2] N.L. Rosi, C.A. Mirkin, Nanostructures in biodiagnostics, Chem. Rev. 105 (2005) 1547–1562.
[3] C. Joachim, J.K. Gimzewski, A. Aviram, Electronics using hybrid-molecular and mono-molecular devices, Nature 408 (2000) 541–548.
[4] D. Cahen, G. Hodes, Molecules and electronic materials, Adv. Mater. 14 (2002) 789–798.

[5] M.F. Garcia-Parajo, G.M.J Segers-Nolten, J.A. Veerman, J. Greve, W.W. Webb, Real-time light-driven dynamics of the fluorescence emission in single green fluorescent protein molecules, Proc. Natl. Acad. Sci. U. S. A. 97 (2000) 7237–7242.
[6] R.M. Dickson, A.B. Cubbitt, R.Y. Tsien, W.E. Moerner, On/off blinking and switching behavior of single molecules of green fluorescent protein, Nature 338 (1997) 355–358.
[7] G. Baldini, F. Cannone, G. Chirico, Pre-unfolding resonant oscillations of single green fluorescent protein molecules, Science 309 (2005) 1096–1100.
[8] F. Cannone, M. Caccia, S. Bologna, A. Diaspro, G. Chirico, Single molecule spectroscopic characterization of GFP-MUT2 mutant for two-photon microscopy applications, Microsc. Res. Tech. 65 (2004) 186–193.
[9] S. Weiss, Fluorescence spectroscopy of single biomolecules, Science 283 (1999) 1676–1683.
[10] M. Bohmer, J. Enderlein, Fluorescence spectroscopy of single molecules under ambient conditions: methodology and technology, ChemPhysChem 4 (2003) 793–808.
[11] E. Haustein, P. Schwille, Single-molecule spectroscopic methods, Curr. Opin. Struck. Biol. 14 (2004) 531–540.
[12] J.N. Forkey, M.E. Quinlam, Y.E. Gordon, Protein structural dynamics by single-molecule fluorescence polarization, Prog. Biophys. Mol. Biol. 74 (2000) 1–35.
[13] G. Jung, J. Wiehler, B. Steipe, C. Bräuchle, A. Zumbusch, Single molecule microscopy of the green fluorescent protein using simultaneous two-color excitation, ChemPhysChem 6 (2001) 392–396.
[14] J.J. Macklin, J.K. Trautman, T.D. Harris, L.E. Brus, Imaging and time-resolved spectroscopy of single molecules at an interface, Science 272 (1996) 255–258.
[15] J.A. Veerman, M.F. Garcia-Parajo, L. Kuipers, N.F. Van Hulst, Time-varying triplet state lifetimes of single molecules, Phys. Rev. Lett. 83 (1999) 2155–2158.
[16] A.G.T. Ruiter, J.A. Veerman, M.F. Garcia Parajo, N.F. Van Hulst, Single molecule rotational and translational diffusion observed by near-field scanning optical microscopy, J. Phys. Chem., A 101 (1997) 7318–7323.
[17] M. Zimmer, Green Fluorescent Protein (GFP): applications, structure, and related photophysical behavior, Chem. Rev. 102 (2002) 759–781.
[18] A.A. Voityuk, M.E. Michel-Beyerle, N. Rosch, Structure and rotation barriers for ground and excited states of the isolated chromophore of the green fluorescent protein, Chem. Phys. Lett. 296 (1998) 269–276.
[19] W. Weber, V. Helms, J.A. McCammon, P.W. Langhoff, Shedding light on the dark and weakly fluorescent states of green fluorescent proteins, Proc. Natl. Acad. Sci. U. S. A. 96 (1999) 6177–6182.
[20] J.D. Badjic, N.M. Kostic, Effects of encapsulation in sol–gel silica glass on esterase activity, conformational stability, and unfolding of bovine carbonic anhydrase II, Chem. Mater. 11 (1999) 3671–3679.
[21] F. Cannone, S. Bologna, B. Campanini, S. Bettati, A. Diaspro, A. Mozzarelli, Tracking unfolding and refolding of single GFPmut2 molecules, Biophys. J. 89 (2005) 2033–2045.
[22] G. Decher, Fuzzy nanoassemblies: toward layered polymeric multi-composites, Science 277 (1997) 1232–1237.
[23] D. Silvano, S. Krol, A. Diaspro, O. Cavalleri, A. Gliozzi, Confocal laser scanning microscopy to study formation and properties of polyelectrolyte nanocapsules derived from CdCO3 templates, Microsc. Res. Tech. 59 (2002) 536–541.
[24] B.C. Cormack, R.H. Valdivia, S. Falkow, FACS-optimized mutants of green fluorescent protein (GFP), Gene 173 (1996) 33–38.
[25] G. Chirico, F. Cannone, S. Beretta, A. Diaspro, B. Campanini, S. Bettati, R. Ruotolo, A. Mozzarelli, Dynamics of Green Fluorescent Protein mutant2 in solution, on spin-coated glasses and encapsulated in nanoporous silica gels, Protein Sci. 11 (2002) 1152–1161.
[26] A. Diaspro, D. Silvano, S. Krol, O. Cavallieri, A. Gliozzi, Single living cell encapsulation in nano-organized polyelectrolyte shells, Langmuir 18 (2002) 5047–5050.
[27] A. Diaspro, S. Krol, R. Magrassi, P. Bianchini, F. Cannone, G. Chirico, C. Palleschi, A. Gliozzi, Encapsulated living cells—bioreactors of the future? Biophys. J. 86 (2004) 625A–626A.
[28] W. Yang, D. Trau, R. Renneberg, N.T. Yu, F. Caruso, Layer-by-layer construction of novel biofunctional fluorescent microparticles for immunoassay applications, J. Colloid Interface Surf. 234 (2001) 356–362.
[29] J.R. Lakowicz, C.D. Geddes, I. Gryczynski, J. Malicka, Z. Gryczynscki, K. Aslan, J. Lukomska, E. Matveeva, J.A. Zhang, R. Badugu, J. Huang, Advances in surface-enhanced fluorescence, J. Fluoresc. 14 (2004) 425–441.
[30] G. Malengo, R. Milani, F. Cannone, S. Krol, A. Diaspro, G. Chirico, High sensitivity optical microscope for single molecule spectroscopy studies, Rev. Sci. Instrum. 75 (2004) 2746–2751.
[31] M.W. Holman, R. Liu, D.M. Adams, Single-molecule spectroscopy of interfacial electron transfer, J. Am. Chem. Soc. 125 (2003) 12649–12654.
[32] W.T. Yip, D.H. Hu, J. Yu, D.A. Vanden Bout, P.F. Barbara, Classifying the photophysical dynamics of single-and multiple-chromophoric molecules by single molecule spectroscopy, J. Phys. Chem., A 102 (1998) 7564–7575.
[33] N.W. Ashcroft, N.D. Mermin, Solid State Physics, 1th ed. Saunders College, Philadelphia, 1976.
[34] C. Tanford, Physical Chemistry of Macromolecules, 2nd ed. John Wiley and Sons Inc., New York, 1963.
[35] S.M. Sze, Physics of Semiconductor Devices, 2nd ed. Wiley, New York, 1981.
[36] T. Blythe, D. Bloor, Electrical Properties of Polymers, 2nd ed., Cambridge University Press, Cambridge (UK), 2005, pp. 27–66, Ch.1.